Optimization of Sphere Population for Electrostatic Multi Sphere Model

Daan Stevenson and Hanspeter Schaub

Simulated Reprint from

12th Spacecraft Charging Technology Conference

Kitakyushu, Japan, May 1418, 2012

Optimization of Sphere Population for Electrostatic Multi Sphere Model

Daan Stevenson and Hanspeter Schaub

***Abstract*—In order to develop robust relative position and orientation control algorithms for Coulomb charge control of spacecraft, accurate but computationally efficient electrostatic models are necessary. The Multi Sphere Model (MSM) predicts the interactions of a charged spacecraft using multiple conducting spheres. In order to improve the accuracy of this model further, a new method is proposed whereby equal radius spheres are placed uniformly on the surface of the spacecraft. The radius is chosen such that the self-capacitance of the MSM is matched to a numerical solution for the conducing shape. The accuracy of this method is verified using a simple system with two spheres, whereby its ability to capture induced charge effects is highlighted. Then, a cylinder-sphere system is analyzed using 105 spheres on the cylinder and 30 spheres on the sphere, providing comparison with a previous three sphere volume populated model for the cylinder. The surface populated model provides much higher accuracy in forces and torques when the separation distances are within 10 craft radii, but there is little improvement outside this range. While the cylinder MSM with three spheres provides force solutions an order of magnitude quicker than the surface MSM method, the setup time for the surface populated MSM is two orders of magnitude faster.**

***Index Terms*—Coulomb charge control, electrostatic modeling**

I. Introduction

A substantial research effort is in progress to determine the feasibility of using Coulomb charge control for relative motion control of nearby spacecraft. Using electron or ion emitters, a spacecraft can accurately control its voltage up to 10s of kV within milliseconds. If the proximity and charge on two craft are sufficient to overcome the local plasma environment, the resultant forces can be utilized to affect their relative position.[1], [2], [3], [4], [5] In the realm of cooperative formation flying missions, this technology provides a benefit over thruster control in its power efficiency and lack of expendable fuel or exhaust plumes. Furthermore, there are some exciting non-cooperative applications for Coulomb charge control, such as electrostatic tugs used to reorbit debris objects.[6], [7], [8]

The drawback that accompanies these benefits of electrostatic actuation is a decrease in controllability. Only one dimension of control is possible per spacecraft body while the resultant electrostatic forces and torques are dictated by the craft shapes, positions and orientations. Moreover, real time knowledge of the exact electrostatic interactions is not possible as there is no analytic solution to Poisson's equation for the potential fields surrounding generic geometries. There are various models that approximate the electrostatics of 3D bodies, each presenting a compromise between accuracy and computational cost, as seen in Figure 1. The highlighted model is the subject of this manuscript, which attempts to bridge the gap in accuracy between previous simplified models and Finite Element Analysis (FEA) approaches, while keeping computational costs low.

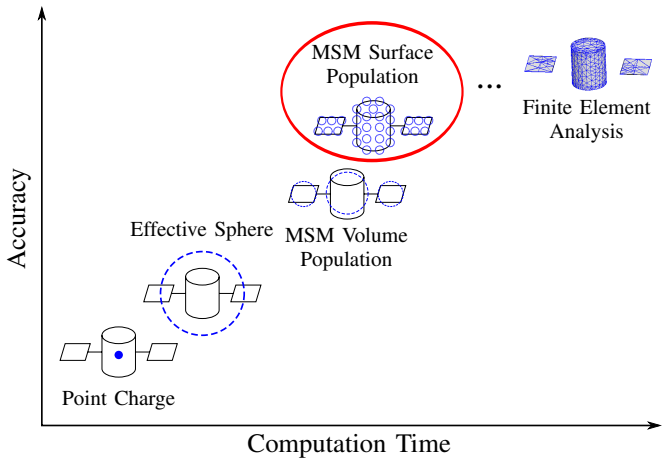

Fig. 1. Comparison of various electrostatic models

The simplest approximation is to treat a spacecraft as a prescribed point charge. This method is used in numerous studies that analyze the relative motion dynamics of Coulomb formations.[9], [10], [11], [12], [13], [14], [15] While the execution of the point charge model is as simple as computing Coulomb's law, it results in a substantial approximation. In actuality, it is not the charge but the voltage that can be controlled on a spacecraft. The total electric charge is then a function of the spacecraft geometry and external potential fields, and is distributed asymmetrically across conducting surface.

An increase in accuracy can be achieved by modeling a spacecraft using an effective sphere with a radius that best represents its electrostatic interaction.[16] When multiple spacecraft are analyzed together, consideration of the Position Dependent Capacitance (PDC) [17] improves knowledge of the voltage to charge relationship throughout the system. One drawback of this approach is that it does not capture the induced charge effects that result from the redistribution of charge within a body in case of small separation distances. For two identical spheres, induced effects can be approximated by certain analytic approaches, but these methods do not expand

D. Stevenson and H. Schaub are with the Colorado Center for Astrodynamics Research, University of Colorado, Boulder, CO 80309-0431, USA (e-mail: daan.stevenson@colorado.edu, hanspeter.schaub@colorado.edu)

to multiple or varying size spheres.

Another limitation of this Effective Sphere Method is its inability to resolve electrostatic torques and non line-of-sight forces that result from non-symmetric spacecraft bodies. This is crucial when relative attitudes and small separation distances on the order of the spacecraft dimensions are a consideration in the mission scenario. The Multi Sphere Model (MSM), as presented in Reference [18], is an approach that attempts to resolve these shortcomings. A generic spacecraft shape is modeled by a collection of conducting spheres. Computation is limited to inverting an $n \times n$ matrix (where n is the number of spheres in the system) to determine the charge on each sphere, and forces and torques are subsequently predicted by summation of the contribution of each sphere by Coulomb's law. This allows for six degree of freedom electrostatic simulations of relative spacecraft motion in real time, which is crucial for the development of robust relative position and orientation control algorithms in local space situational awareness applications.

At the most accurate end of the spectrum, FEA software such as Ansoft's Maxwell 3D ©,[19] creates a highly precise but computationally expensive solution of the electrostatic potential fields by solving Poisson's equation on each finite element in the entire 3D space, with boundary conditions created from the spacecraft geometries and potentials. FEA solvers are not capable of faster-than-realtime charged relative motion simulations, and therefore do not provide analytical insight into the dynamics and control of such scenarios. They are, however, useful for creating truth solutions that can be used to verify the lower order models of interest here.

The prior MSM scheme that attempt to populate the spacecraft volume with interior spheres is referred to as the Volume MSM, or VMSM. Here a nonlinear fit is used to match the forces and torques from a truth model as described above at various separation distances and orientations. One drawback of this VMSM approach is the necessity for an external shape to generate forces and torques. Another limitation is that, despite implementing symmetry arguments, the nonlinear fit is not robust for increasing numbers of spheres, which is desirable to capture the 3D and induced charge effects of more intricate geometries at small separation distances. This paper will investigate how to populate generic spacecraft shapes with higher numbers of uniformly positioned spheres, placed on the surface of the conducting body. This method is referred to as the Surface MSM, or SMSM. There is a slightly higher computational cost when computing forces and torques due to the increase in size of the Position Dependent Capacitance matrix, but the time necessary to set up the model is dramatically decreased. In the end, this new method helps to bridge the gap in accuracy between the original MSM and FEA approaches. Meanwhile, none of the models discussed above are rendered obsolete by the inclusion of a new approach, if the trade-offs of computation time and accuracy are considered. Rather, the new SMSM method provides a new tool for scenarios where increased electrostatic force and torque modeling is critical for single digit craft radii separation distances.

II. Multi Sphere Model Methodology Review

In order to discuss the new method for populating spheres on the surface of a spacecraft body, the general Multi Sphere Model is reviewed. The novel SMSM research addresses how the size and location of spheres are chosen. Once this is accomplished, computing forces and torques on the bodies in the system is equivalent to the original methodology proposed in Reference [18]. A rigid spacecraft or space debris object is modeled by a collection of spheres with fixed sizes and relative positions, as shown in Figure 2. Satellite A is modeled by 4 spheres, while object B happens to be represented by a single sphere.

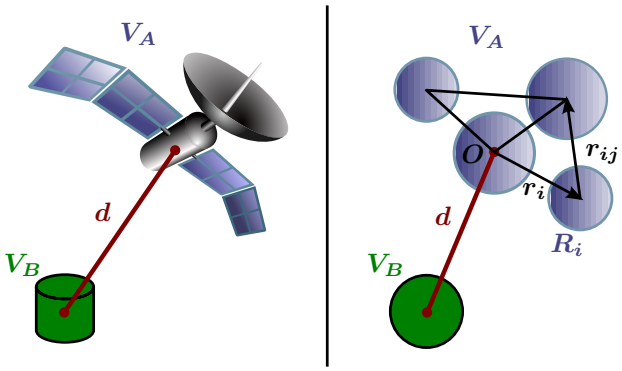

Fig. 2. Conceptual depiction of Multi Sphere Method

While the absolute electrostatic voltage is assumed to be prescribed on a spacecraft, the Coulomb force between the spheres depends on the charge that each holds. The voltage V_i on a given sphere is a result of both the charge on that sphere and the charges on its neighboring spheres. This relation is given in Eq. (1), [17], [20] where R_i represents the radius of the sphere in question and $\boldsymbol{r}_{i,j} = \boldsymbol{r}_j - \boldsymbol{r}_j$ is the center-to-center distance to each neighbor. The constant $k_c = 8.99 \times 10^9$ Nm^2/C^2 is Coulomb's constant, and q_i stands for the charge on a given sphere.

$$V_i = k_c \frac{q_i}{R_i} + \sum_{j=1, j\neq i}^{m} k_c \frac{q_j}{r_{i,j}} \tag{1}$$

The linear relations for each of the $m = n + 1$ spheres in the system (n spheres in the MSM plus the external sphere) can be combined in the matrix form of Eq. (2), where $\boldsymbol{V} = [V_A, V_A, ..., V_A, V_B]^T$ and $\boldsymbol{q} = [q_1, q_2, ..., q_n, q_B]^T$ represent matrix collections of the voltages and charges in the entire system.

$$\boldsymbol{V} = k_c [C_M]^{-1} \boldsymbol{q} \tag{2}$$

Note that V_A is the prescribed voltage on all spheres in the model while the external sphere is held at V_B. The effects of varying the voltage on different spheres within the model have not been analyzed, but keeping the voltage constant is logical since the modeled conducting spacecraft would be held at uniform voltage. This approach also reduces the amount of model parameters.

The inverse of the Position Dependent Capacitance (PDC) matrix in Eq. (2), $[C_M]^{-1}$, can be expanded as follows, according to the nomenclature adopted in Figure 2, with $\boldsymbol{r}_{i,B} = \boldsymbol{d} - \boldsymbol{r}_i$:

$$[C_M]^{-1} = \begin{bmatrix} 1/R_1 & 1/r_{1,2} & \cdots & 1/r_{1,n} & 1/r_{1,B} \\ 1/r_{2,1} & 1/R_2 & \ddots & \vdots & \vdots \\ \vdots & \ddots & \ddots & \vdots & \vdots \\ 1/r_{n,1} & \cdots & \cdots & 1/R_n & 1/r_{n,B} \\ 1/r_{B,1} & \cdots & \cdots & 1/r_{B,n} & 1/R_B \end{bmatrix} \tag{3}$$

The next step is to solve for the array of charges $\boldsymbol{q}$ from Eq. (2) by inverting this $n+1$ size symmetric matrix, a computation that becomes increasingly intensive when more spheres are used in the model. Coulomb's law can then be implemented to calculate the linear force between each charged sphere. Since the location of the spheres within the modeled body are held fixed with respect to each other, their equal and opposite contributions cancel. The total force $\boldsymbol{F}$ and torque $\boldsymbol{L}$ about the origin O on body A due to external shape B is then given by the following summations:

$$\boldsymbol{F}_O = k_c q_B \sum_{i=1}^{n} \frac{q_i}{{r_{i,B}}^3} \boldsymbol{r}_{i,B} \tag{4}$$

$$\boldsymbol{L}_O = k_c q_B \sum_{i=1}^{n} \frac{q_i}{{r_{i,B}}^3} \boldsymbol{r}_i \times \boldsymbol{r}_{i,B} \tag{5}$$

While any origin can be chosen for body A, the force and torque in Eqs. (4) and (5) are now defined from this reference origin. If the object B is modeled by another MSM, the force and torque relations contain double summations.

III. Surface Population Motivation

During previous developments, three spheres are used to model a cylinder shape. While considering symmetry of the original geometry, the size and position of each sphere is determined by fitting to the numerically solved force and torque values on the cylinder in the presence of a charged external sphere. While this volume based sphere population works well to predict the electrostatic interactions of the cylinder shape, capturing the 3D and induced charge effects of more intricate geometries at small separation distances will require a model with more than three spheres. The MSM algorithm for calculating forces and torques can handle models with large numbers of spheres, but the nonlinear fitting schemes used to optimize the sphere positions and sizes are not robust in this domain. As with any nonlinear fitting algorithm, when the parameter set increases, successful convergence is dependent on the chosen initial conditions and global optimization is not guaranteed.

For this reason, expanding the MSM to higher accuracy levels requires populating the spacecraft shape with an increasing number of uniformly positioned spheres. This leads to a higher fidelity prediction of the electrostatic interactions because the charge has a higher degree of freedom to move between the various spheres in the model, much like it would on the actual conducting shape. In this way, induced charge effects can be captured in any dimension where multiple spheres are present. Since the underlying assumption that the modeled body is fully conducting remains, it is known that all the contained charge will reside on its surface. Therefore, the approach is taken to populate only the *surface* of a given shape with spheres.

The goal of the new method of surface population is to minimize the parameters that need to be selected when creating an MSM for a given shape. Therefore, it is desirable to pick a set of spheres that are *uniformly* distributed along the surface of the geometry. For complex shapes this is not a trivial task. Several CAD programs contain algorithms to generate point clouds from solid models and this is most likely the approach that will be taken during future work for generating sphere positions for generic spacecraft. For simpler shapes such as spheres and cylinders, specific algorithms are created to uniformly populated the surface as described below. By this approach, the new SMSM method is significantly faster and more robust to set up. The resulting computations are more accurate, while the run-time costs are only marginally increased.

IV. Two Sphere System

To analyze the quality of a uniform surface populated MSM, simple shapes are used to provide benchmark performance results. An isolated sphere in space has an analytic solution for its self-capacitance, and for a system with two spheres separated at appreciable distances the Position Dependent Capacitance model can predict Coulomb forces fairly accurately. For smaller separation distances, several analytic and numerical options exist that can be used as accurate truth models. By comparing these truth models with the PDC solution, it is easy to isolate the contribution from induced charge effects.

A. Uniform Population on a Sphere

To model the two sphere system with the MSM, the goal is to uniformly populate the surface of a sphere with equidistant points, which is a well documented computer science problem.[21] Coincidentally, the most robust algorithms involve equal electrostatic repulsion of the points, which could be used to generate surface points for generic shapes in later research. For the current effort, a Golden Section Spiral distribution provides sufficiently uniform spacing of points. The sphere is divided into parallel bands of equal area, and points are placed along the spiral at successive longitudes such that their ratio is the most irrational golden ratio, resulting in the golden angle:

$$\psi = \pi(3 - \sqrt{5}) \tag{6}$$

Figure 3 shows the resulting sphere population for $n = 4, 10$ and 30 spheres.

B. Optimal Packing Parameter

With the spheres in the MSM positioned in a uniform manner on the surface of the modeled geometry, the one remaining parameter to choose is the spheres' radius R, which

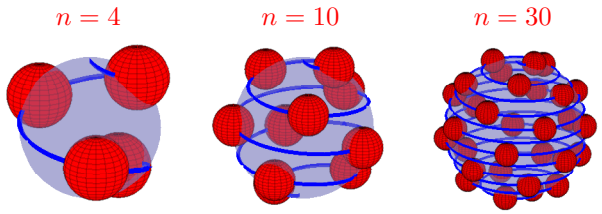

Fig. 3. Various uniform point distributions on the surface of a sphere

is assumed constant throughout the SMSM model. While the goal is ultimately to match Coulomb forces and torques with external objects, only one scalar invariant quantity is necessary to determine an optimal radius. In contrast to the VMSM method where increasing numbers of sphere locations and radii must be chosen as the number of spheres increases, the SMSM method only needs to determine a single parameter R. This provides a significant simplification of the model development with a large number of spheres. The self-capacitance of a conducting geometry in space is a good candidate empirical quantity to be used to determine the optimal sphere radius R.

For a modeled sphere with radius R_S, the self-capacitance C is analytically known:

$$C_{\text{sphere}} = \frac{R_S}{k_c} \tag{7}$$

Meanwhile, the capacitance of the MSM can be computed by summation of the charge q_i on each sphere in the model (as determined by the process in Section II) for a given voltage V:

$$C_{\text{MSM}} = \frac{Q}{V} = \frac{\sum_{i=1}^{n} q_i}{V} \tag{8}$$

A simple optimizing function based on a golden section search and parabolic interpolation is used to choose a radius R that minimizes

$$f(R) = C_{\text{MSM}} - C_{\text{sphere}} \tag{9}$$

This is performed for various n numbers of spheres in the model.

In order to analyze the optimal sphere size across various geometries, comparing the total surface area $4\pi R^2 n$ of every sphere in the MSM to the total surface area S of the modeled geometry provides geometric insight. This relation is represented by the packing parameter γ:

$$\gamma = \frac{4\pi R^2 n}{S} \tag{10}$$

For the benchmark spherical spacecraft case being modeled with the SMSM, the optimal packing parameter is plotted against the number of spheres in the model in Figure 4. Interestingly, even though the number of spheres in the model and therefore the spacing between them changes, the parameter γ appears to converge to a constant value.

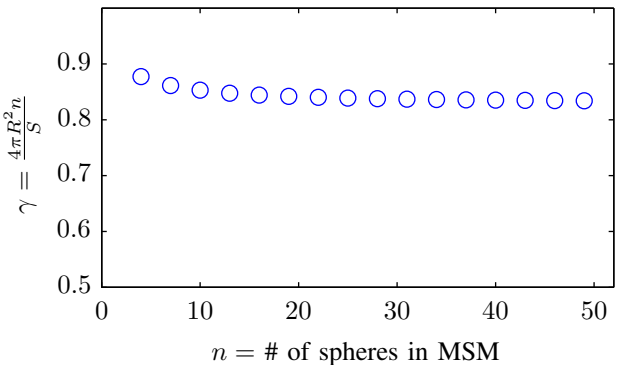

Fig. 4. Optimal packing parameter for surface MSM on sphere

C. Truth Models

While the radii of the spheres in the model are optimized as above to match the self-capacitance of the modeled sphere, validation requires that the resultant electrostatic forces match those from analytic and numerical solutions. A simple system is used that consists of two spheres with radii $R_S = 0.5$ m, various separation distances d, and equal as well as opposite sphere voltages $V = \pm 30$ kV. Maxwell 3D is used to provide a numerical answer. The mesh and charge distribution in Maxwell is visible in Figure 6(a) of the following section.

The simplicity of the two sphere system lends itself to several analytic solutions. The PDC model for two spheres captures the relationship between the prescribed voltage and the total charge on each sphere, but not the induced charge effects. If each sphere is modeled with a single charge at its center, the resulting voltage in space is not constant at the sphere boundaries, as it would be on a conducting body. The two approaches in Figure 5 attempt to offset this anomaly by ensuring that the spheres form equipotential surfaces. They are valid only for a system where both conducting spheres are of equal radius and are held at equal magnitude voltages, as is the case here.

The first order induced charge model, shown in Figure 5(a), attempts to capture induced effects by a one dimensional change in separation distances. The separation d between the charges q_A and q_B that are computed using the PDC, is adjusted by an extra distance x. This distance is chosen such that V_L and V_R are equal, resulting in a cubic equation in x.[22] The figure shows an increased separation as for the repulsion case; attraction would result in a decreased separation distance.

In Soules' Method of Images (MOI), illustrated in Figure 5(b), successively smaller image charges q_i are placed at distances x_i along the line of centers to approximate the induced charged distribution:[23]

$$q_i = \pm \frac{r q_{n-1}}{d - x_{n-1}} \tag{11a}$$

$$x_i = \frac{{R_S}^2}{d - x_{n-1}} \tag{11b}$$

Here $n > 1$, q_1 is determined for a given voltage using the PDC, and $x_1 = 0$. In Equation (11b), the successive charges switch polarity $(-)$ for the repulsion case and maintain the same polarity $(+)$ for attraction. In the case of an infinite series of charges, the result is claimed to approach an exact formula for the same system as derived by Maxwell using zonal harmonics.[20] The algorithm is implemented using 19 spheres as in Reference [22].

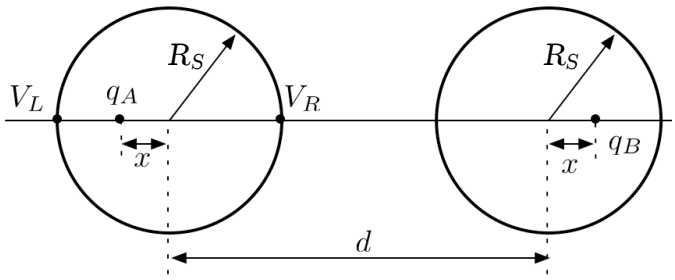

(a) First order induced charge model (repulsion)

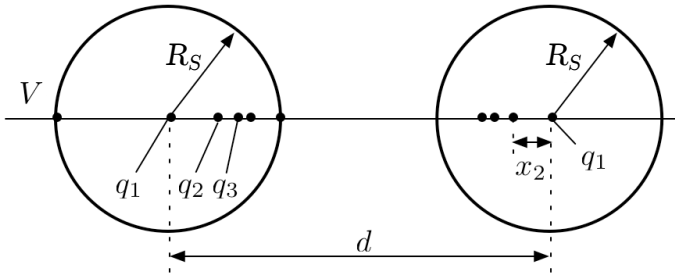

(b) Electrostatic Method of Images

Fig. 5. Two analytic models for the two sphere system that capture induced effects

While the two induced charge models discussed above provide a vast improvement over the PDC in force prediction at small separation distances, Maxwell 3D is found to produce the most accurate solution when the simulation is tuned properly. Therefore the Maxwell solution is used as the truth model for verification of the surface populated Multi Sphere Model.

D. Force Comparison

This system discussed above is depicted in Figure 6 with the charge density distribution shown in both Maxwell 3D and on a 30 sphere surface populated MSM. This qualitatively highlights the ability of the SMSM to capture induced charge effects when enough spheres are present on the object surface. In order to offset the difference in surface areas, the charge density σ_i on each sphere in Figure 6(b) is normalized by the factor γ from Eq. (10):

$$\sigma_i = \gamma \frac{q_i}{4\pi {R_i}^2} \tag{12}$$

Radii for the models are chosen to fit capacitance of the sphere as above, resulting in

$$R \text{ (10 spheres)} = 0.1460 \text{ m} \tag{13}$$

$$R \text{ (30 spheres)} = 0.0835 \text{ m} \tag{14}$$

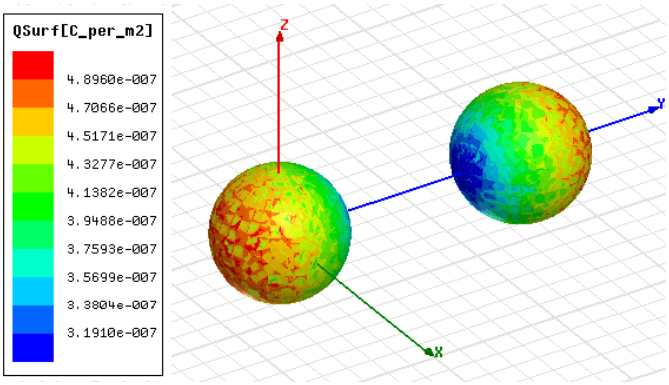

(a) Maxwell 3D

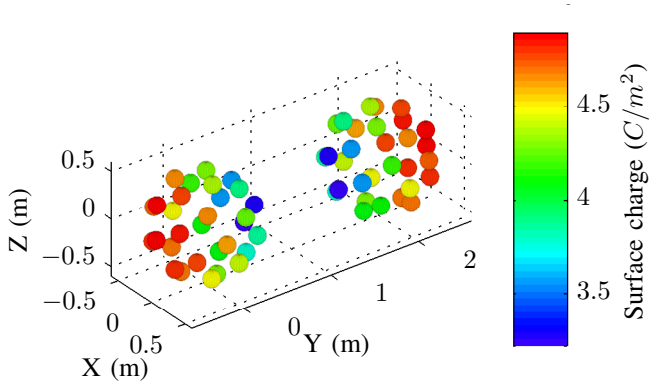

(b) MSM with 30 spheres

Fig. 6. Charge density distribution on two spheres ($V_1 = V_2 = +30$ kV)

Figure 7 gives the percent error for various models at a range of separation distances, for the attractive and repulsive cases (7(b) & 7(b), respectively). Percent error is defined as

$$Err = \frac{F_{\text{model}} - F_{\text{Maxwell}}}{F_{\text{Maxwell}}} \tag{15}$$

The PDC model produces almost 50% error at very small separation distances, but matches the full solution well at further distances. Using the Maxwell solution as the truth model, it is surprising that there is a discrepancy between it and the Method of Images solution, as this should closely represent the full analytic solution according to Reference [20]. As more spheres are added to the MSM, however, the errors at close distances converge to zero, thus giving further credence to the solution given by Maxwell 3D. The first order induced charge method matches Maxwell for the repulsion case but is equivalent to the Method of Images for the attractive case, which is likely a coincidence.

The SMSM with 30 spheres results in less than a percent error for repulsion right up to where the spheres touch at $d = 2R_S$. For attraction, induced effects are known to be even

more dominant, and more spheres are necessary to completely capture these effects. The PDC model shows nearly twice as much error as for the repulsion case. The 10 sphere SMSM results in up to 40% error as the spheres nearly touch, but this drops off quickly to less than 2% when $d = 3.5R_S$. All in all, the surface populated MSM is clearly shown to model the electrostatic interactions of the spheres to a very high degree of accuracy. It provides a more accurate solution than other induced charge effect models, while increasing in accuracy as more spheres are added. Moreover, this method is expandable to generic spacecraft shapes where the others are not.

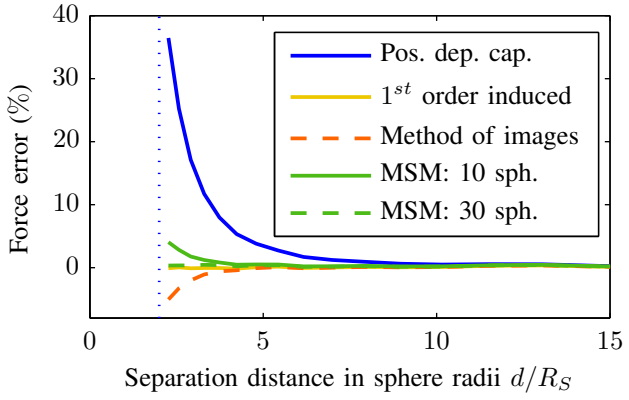

(a) Repulsive Forces ($V_1 = +30$ kV, $V_2 = -30$ kV)

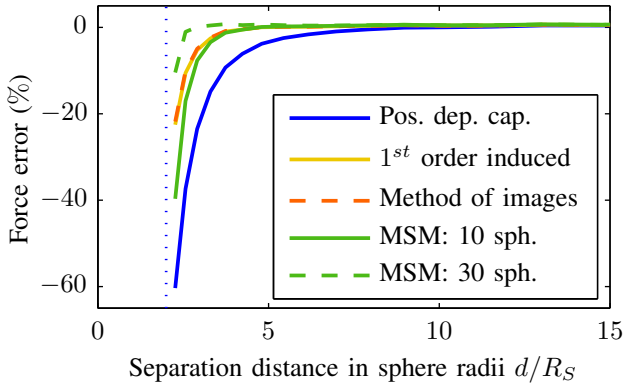

(b) Attractive Forces ($V_1 = V_2 = +30$ kV)

Fig. 7. Error in force between two spheres for various electrostatic models

These results beg the question, how does the uniform sphere radius R, and thus the packing parameter $\gamma = \frac{4\pi R^2 n}{S}$, affect the resulting force computations? In Figure 7, this parameter is optimized such that the capacitance of the MSM matches the capacitance of the sphere that it is intended to model. If a different R is chosen, might the model match the true forces better at close separation distances? Figure 8 shows the error in force at three separation distances, for a range of γ values, comparing both the 10 and 30 sphere model. The repulsion configuration is chosen with $V_1 = V_2 = +30$ kV.

At the larger separation distance ($d = 15R_S$), the force error is minimized when $\gamma = 0.8464$ for $n = 10$ and when $\gamma = 0.8273$ for $n = 30$, as shown by the red circle. This

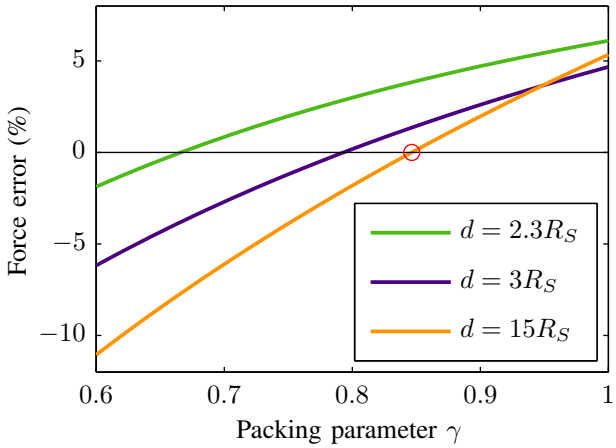

(a) MSM with 10 spheres

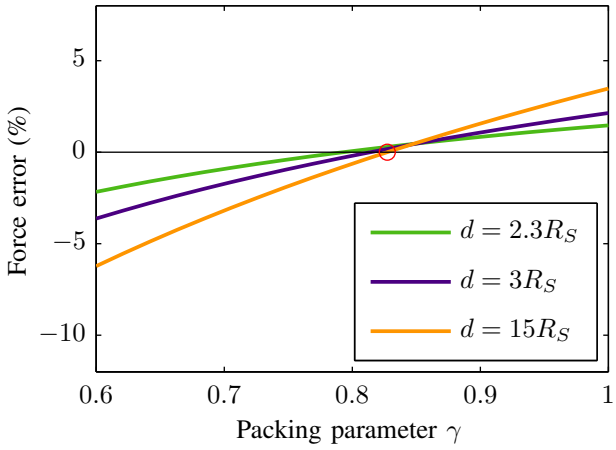

(b) MSM with 30 spheres

Fig. 8. Error in force for various packing parameters

corresponds within a fraction of a percent to the optimal values in Figure 4, suggesting that fitting the model-sphere radii to the body capacitance results in the optimal force prediction at larger separation distances. To match the induced charge effects and forces at closer distances, the optimal packing parameter γ (and therefore R) is smaller. Choosing R on this basis, however, would result in significant errors at larger separation distances. In the end, spacecraft proximity missions would rarely operate at fewer than 10 craft radii separation unless docking is considered, so the best approach is to choose the sphere radii by matching to the spacecraft body's self-capacitance in deep space as outlined in Section IV-B. Notice that the sensitivity in force error to γ is appreciably decreased for the model with more spheres, which is a promising feature of the new method.

V. Surface MSM Methodology for Generic Spacecraft Shape

With the accuracy of the new model sufficiently verified for simple shapes, it can be applied to model spacecraft

with arbitrary 3D shapes. Before the results for such shapes are analyzed, the methodology for determining the sphere parameters for a generic spacecraft shape is given in Figure 9. The red boxes are processes that must be executed when analytic solutions are not present for the sphere distribution and capacitance, as is most often the case. The two components of a full MSM are the location $\boldsymbol{r_i}$ and radii R_i of each sphere. For a generic body, a solid modeling program will be necessary to determine a uniform point cloud model on the surface. For most shapes, the capacitance is to be found by an electrostatic modeling program such as Maxwell 3D. The Position Dependent Capacitance matrix is then used to calculate the capacitance for the system of spheres to determine an optimal uniform radius R that matches the capacitance from the numerical solution. At this point, the full model can be used in conjunction with other MSM objects to determine the electrostatic interactions.

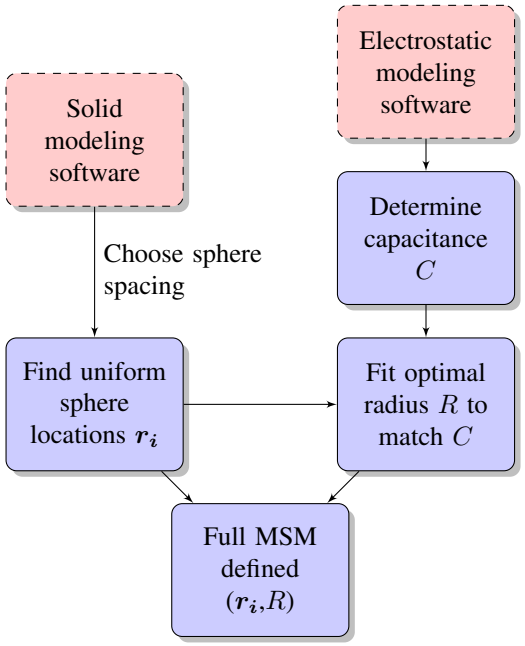

Fig. 9. Methodology for parameter selection of surface populated MSM

VI. Cylinder Model Results

A. Setup

In Reference [18], where the MSM was first introduced, the interaction between a 3 m length by 1 m diameter cylinder and a 1 m diameter sphere are used to determine optimal sphere parameters and verify the model. Collecting force and torque values at various separation distances and orientations provides invaluable insight into the ability of a model to replicate induced charge effects, 3D effects, and large distance behaviors. The same approach is implemented to verify the surface populated Multi Sphere Model and compare it to the three sphere model from the previous research. Using a set of Maxwell data that ranges to 20 m separation distance, the model in Figure 10 is generated, with parameters given in Table I. Note that in comparison with the setup outlined in Figure 9, choosing parameters for this three sphere model necessitates collecting a full sweep of Maxwell truth data, followed by a difficult to implement nonlinear fit.

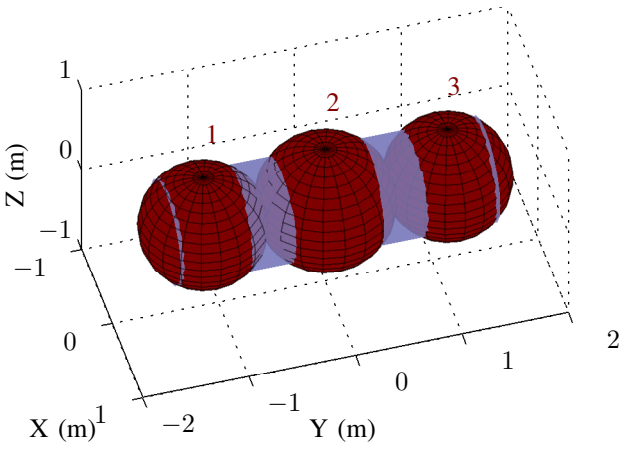

Fig. 10. Multi Sphere Model parameters for cylinder geometry

TABLE I
Parameters of three sphere MSM for cylinder

	Sphere 1	Sphere 2	Sphere 3
X Coordinate (m)	0	0	0
Y Coordinate (m)	-1.1454	0	1.1454
Z Coordinate (m)	0	0	0
Radius (m)	0.5959	0.6534	0.5959

Now the methodology in Figure 9 is implemented. Since the cylinder is still a fairly simple shape, manual algorithms are used to populate the surface. For the end discs, a gold section spiral is utilized much like for populating the spheres in Figure 3, while on the circumference of the body, a hexagonal packing is implemented. Maxwell is used to determine that the self capacitance of the cylinder in space is

$$C_{\text{cylinder}} = 1.0616 \times 10^{-10} \frac{C}{V} \tag{16}$$

This is used to fit the optimal sphere radius, resulting in Figure 11, which shows the packing parameter γ as a function of the total number of spheres n in the cylinder model. Clearly, the optimal γ values do not match those for the sphere in Figure 4. For this reason, R must be fit for a specific sphere distribution to match the capacitance of a given model shape.

A cylinder model with $n = 105$ spheres ($R = 0.0731$ m) and a sphere model with $n = 30$ spheres as above ($R = 0.0835$ m) is depicted in Figure 12. Each is held at $V = +30kV$ and the induced charge effects are clearly visible from the charge distribution throughout the shapes.

B. Results

Figure 13 and 14 show the accuracy of the force and torque, respectively, calculated by the VMSM model with

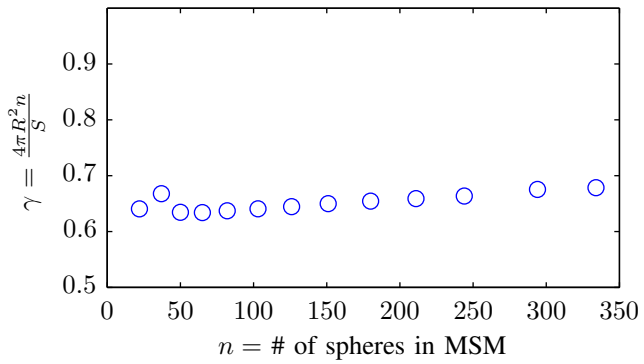

Fig. 11. Optimal packing parameter for Surface MSM on cylinder

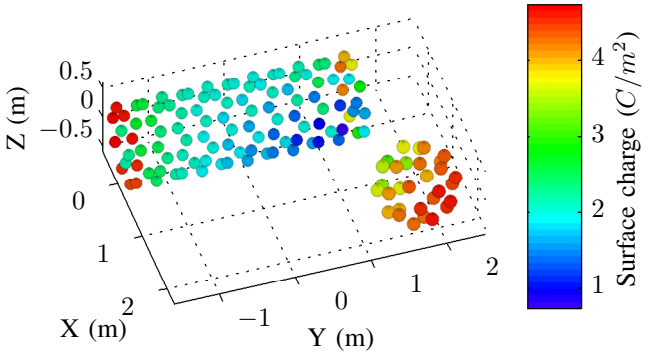

Fig. 12. Charge density distribution on SMSM of cylinder and sphere ($V_1 = V_2 = +30$ kV)

three spheres and the surface populated model (105 spheres in the cylinder and 30 spheres in the sphere), compared to the truth data from Maxwell. Figure 13(a) is a 1 to 1 plot between the MSM models and the Maxwell data, where the black line represents perfect matching between the two models. The three sphere VMSM over-predicts the larger forces that correspond to small separation distances. The drawback of this visualization is that it isn't possible to see where in relation to the cylinder the sphere is located for a given data point. Figure 13(b) and 13(c) rectify this shortcoming, as they show the absolute force errors compared to Maxwell, for the three sphere and surface populated MSM, respectively. A representative size cylinder and sphere are included for reference, while the color legend is in logarithmic scale. The same organization is used in Figure 14 for the torques exerted on the cylinder.

It is clear from the figures that the SMSM predicts the forces much better at small separation distances across the range of angles, but by about 6 m separation (12 craft radii), the difference between the two models is fairly negligible. For the case of torques, the three sphere model actually does a slightly better job at separation distances larger than 4 m (8 craft radii). This is likely because the volume populated model is fit directly to the Maxwell data, which has been shown earlier to exhibit some accuracy discrepancies at this range. Regardless, most Coulomb charge control applications that don't involve docking occur at separation distances beyond this range.

It is important to weigh the accuracy with computation and setup times of the different models, as shown in Table II. The first column gives the time for each model to compute a force and torque value at each of the 82 relative positions. While this computation takes Maxwell about 1 hour and 14 minutes at fairly moderate accuracy settings, the MSM with three spheres completes the task in a fraction of a second. Meanwhile, it takes the surface populate model (with 135 spheres in the system) about 16 seconds. The next column shows the numerical calculation time necessary for the setup of the two MSM models. For the volume populated (3-sphere) MSM, this requires the complete set of data calculated earlier by Maxwell, while the surface populated MSM only requires a single numerical computation of the capacitance of the body. The 'Fit' column represents the nonlinear numerical fit for the 3-sphere VMSM, and determination of the sphere positions as well as a fit to match R to capacitance for the surface populated model. As is clear, computation happens about an order of magnitude quicker for the VMSM, but setup is two orders of magnitude quicker for the new model. Depending on the requirements on accuracy and computation time, both models are viable candidates for use in the calculation of spacecraft electrostatic interactions. Both exceed Maxwell 3D or other finite element analysis software in the ability to predict forces and torques in real time.

TABLE II
SETUP AND COMPUTATION TIME FOR CALCULATION OF FORCE AND TORQUES BETWEEN SPHERE AND CYLINDER AT 82 RELATIVE LOCATIONS

[Time in sec]	Comp.	Setup				
Maxwell	4434	Num.		Fit		Total
3-sph VMSM	**0.11**	4434	+	9.1	=	**4443.1**
Surface MSM	**15.6**	54.1	+	4.1	=	**58.2**

VII. CONCLUSION

In an attempt to increase the accuracy of the Multi Sphere Model (MSM) while avoiding the complicated nonlinear parameter fit, a new surface sphere population method is created. Spheres are uniformly placed on the surface of a modeled spacecraft shape, while the common sphere radius is chosen to match the numerically determined capacitance of the conducting object. This greatly reduces the setup time for the MSM (by two orders of magnitude), while the computation time is slightly increased due to the larger number of spheres (one order of magnitude). The result is a model that captures small separation distance induced charge effects very successfully, nearing the accuracy in electrostatic force and torque calculation of full Finite Element Analysis (FEA) software. Initial verification is performed using a simple system with two spheres, for which numerical and analytical solutions are available as truth models. The surface populated MSM

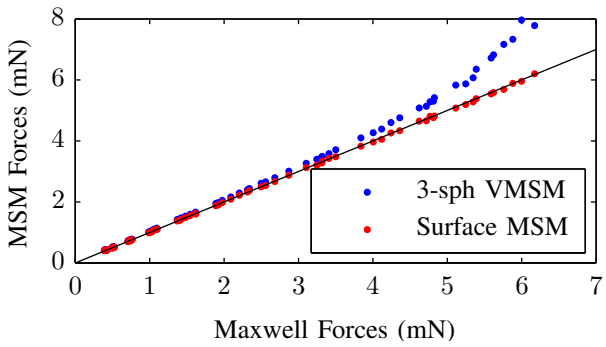

(a) Both models compared to Maxwell

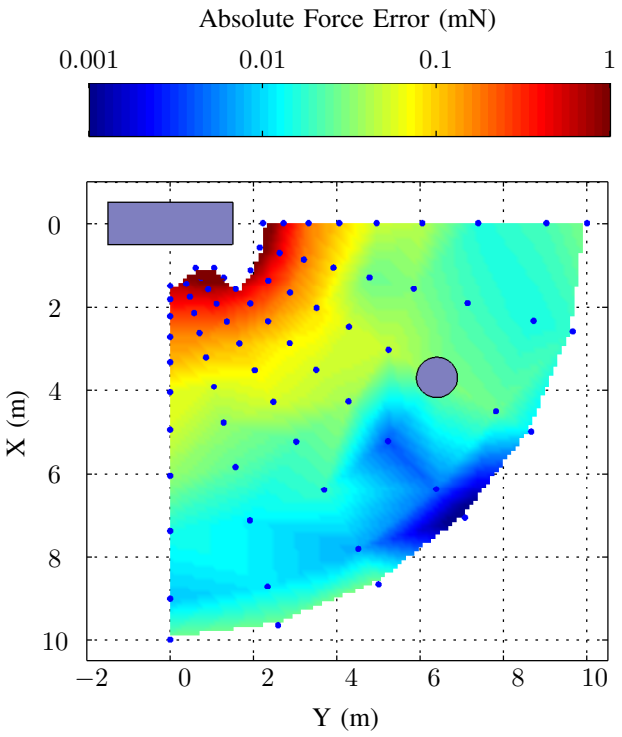

(b) 3-sphere VMSM Errors

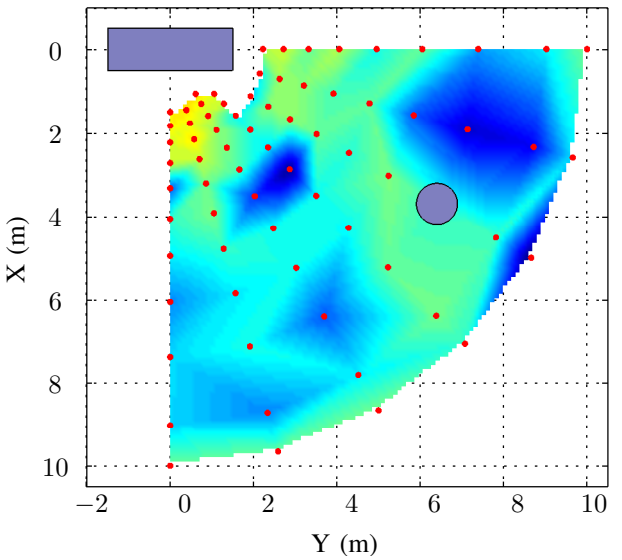

(c) Surface MSM Errors

Fig. 13. Force comparison between MSM models and Maxwell

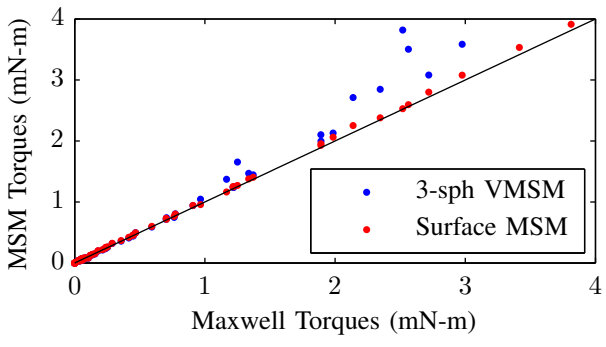

(a) Both models compared to Maxwell

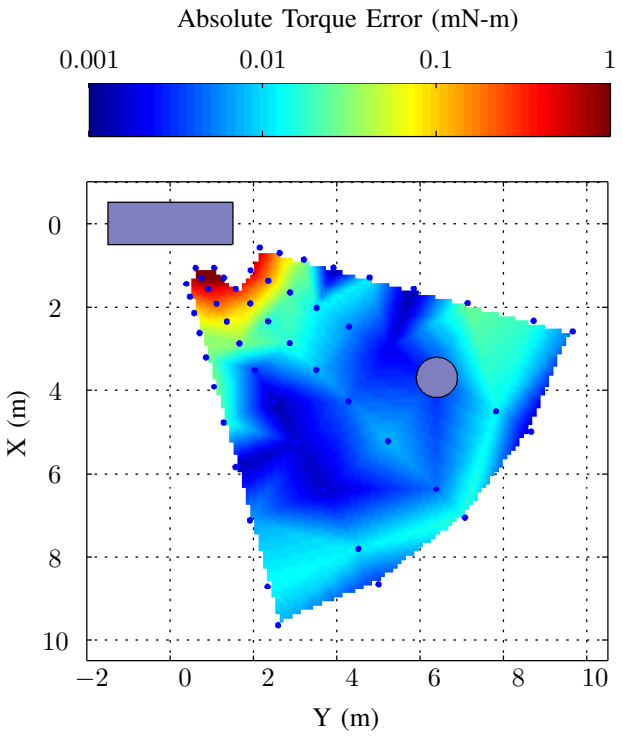

(b) 3-sphere VMSM Errors

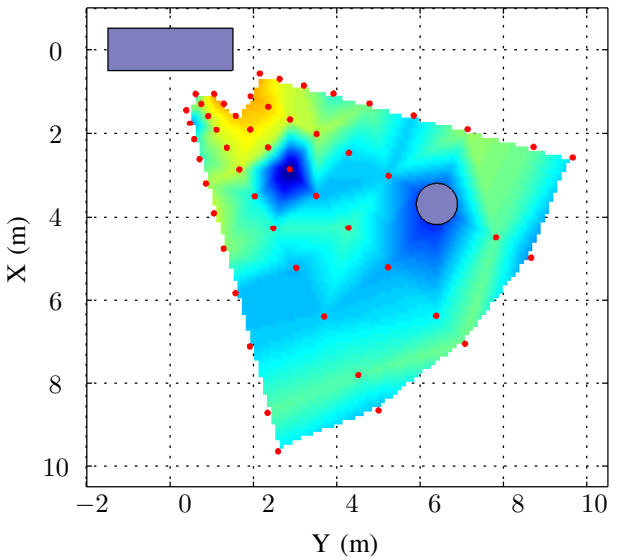

(c) Surface MSM Errors

Fig. 14. Torque comparison between MSM models and Maxwell

converges to a full FEA solution for increasing numbers of spheres, even as separation distances become especially small. Next, forces and torques on a cylinder are examined, showing that the increase in spheres from the three sphere MSM to a 105 sphere surface MSM results in a vast improvement in accuracy up to about 10 craft radii separation distance, outside of which both models perform equally well.

ACKNOWLEDGMENT

This material is based upon work supported by the NASA Science & Technology Research Fellowship (NASA Grant #NNX11AN47H).

REFERENCES

[1] L. B. King, G. G. Parker, S. Deshmukh, and J.-H. Chong, "Spacecraft formation-flying using inter-vehicle coulomb forces," NASA/NIAC, Tech. Rep., January 2002, http://www.niac.usra.edu.

[2] ——, "Study of interspacecraft coulomb forces and implications for formation flying," *AIAA Journal of Propulsion and Power*, vol. 19, no. 3, pp. 497–505, May–June 2003.

[3] H. Schaub, G. G. Parker, and L. B. King, "Challenges and prospect of coulomb formations," *Journal of the Astronautical Sciences*, vol. 52, no. 1–2, pp. 169–193, Jan.–June 2004.

[4] A. C. Tribble, *The Space Environment - Implications for Spacecraft Design*, revised and expanded ed. Princton University Press, 2003.

[5] M. H. Denton, M. F. Thomsen, H. Korth, S. Lynch, J. C. Zhang, and M. W. Liemohn, "Bulk plasma properties at geosynchronous orbit," *Journal of Geophysical Research*, vol. 110, no. A7, 07 2005. [Online]. Available: http://dx.doi.org/10.1029/2004JA010861

[6] H. Schaub and D. F. Moorer, "Geosynchronous large debris reorbiter: Challenges and prospects," in *AAS Kyle T. Alfriend Astrodynamics Symposium*, Monterey, CA, May 17–19 2010, paper No. AAS 10-311.

[7] H. Schaub and L. E. Z. Jasper, "Circular orbit radius control using electrostatic actuation for 2-craft configurations," in *AAS/AIAA Astrodynamics Specialist Conference*, Girdwood, Alaska, July 31 – August 4 2011, Paper AAS 11–498.

[8] E. Hogan and H. Schaub, "Relative motion control for two-spacecraft electrostatic orbit corrections," in *AAS/AIAA Spaceflight Mechanics Meeting*, Girdwood, Alaska, July 31 – August 4 2011, Paper AAS 11–466.

[9] J. Berryman and H. Schaub, "Analytical charge analysis for 2- and 3-craft coulomb formations," *AIAA Journal of Guidance, Control, and Dynamics*, vol. 30, no. 6, pp. 1701–1710, Nov.–Dec. 2007.

[10] H. Vasavada and H. Schaub, "Analytic solutions for equal mass four-craft static coulomb formation," *Journal of the Astronautical Sciences*, vol. 56, no. 1, pp. 17–40, Jan. – March 2008.

[11] E. Hogan and H. Schaub, "Collinear invariant shapes for three-craft coulomb formations," *Acta Astronautica*, vol. 12, pp. 78–89, March–April 2012.

[12] G. G. Parker, C. E. Passerello, and H. Schaub, "Static formation control using interspacecraft coulomb forces," in *2nd International Symposium on Formation Flying Missions and Technologies*, Washington D.C., Sept. 14–16, 2004 2004.

[13] H. Schaub, C. Hall, and J. Berryman, "Necessary conditions for circularly-restricted static coulomb formations," *Journal of the Astronautical Sciences*, vol. 54, no. 3–4, pp. 525–541, July-Dec. 2006.

[14] H. Schaub, "Stabilization of satellite motion relative to a coulomb spacecraft formation," *Journal of Guidance, Control and Dynamics*, vol. 28, no. 6, pp. 1231–1239, Nov.–Dec. 2005.

[15] A. Natarajan and H. Schaub, "Linear dynamics and stability analysis of a coulomb tether formation," *Journal of Guidance, Control, and Dynamics*, vol. 29, no. 4, pp. 831–839, July–Aug. 2006.

[16] L. E. Z. Jasper and H. Schaub, "Effective sphere modeling for electrostatic forces on a three-dimensional spacecraft shape," in *AAS/AIAA Spaceflight Mechanics Meeting*, Girdwood, Alaska, July 31 – August 4 2011, Paper AAS 11–465.

[17] W. R. Smythe, *Static and Dynamic Electricity*, 3rd ed. McGraw–Hill, 1968.

[18] D. Stevenson and H. Schaub, "Multi sphere modeling for electrostatic forces on three-dimensional spacecraft shapes," in *AAS/AIAA Spaceflight Mechanics Meeting*, Charleston, South Carolina, Jan. 29 – Feb. 2 2012, Paper AAS 12-106.

[19] ANSYS, *Maxwell 3D Software*, 2010, version 13.0.0. http://www.ansoft.com/products/em/maxwell.

[20] J. Sliško and R. A. Brito-Orta, "On approximate formulas for the electrostatic force between two conducting spheres," *American Journal of Physics*, vol. 66, no. 4, pp. 352–355, 1998.

[21] P. Boucher. (2006, Obtober) Points on a sphere @ONLINE. [Online]. Available: http://www.softimageblog.com/archives/115

[22] C. R. Seubert and H. Schaub, "Electrostatic force model for terrestrial experiments on the coulomb testbed," in *61st International Astronautical Congress*. Prague, CZ: International Astronautical Federation, Sept. 2010, paper IAC-10.C1.1.9.

[23] J. A. Soules, "Precise calculation of the electrostatic force between charged spheres including induction effects," *American Journal of Physics*, vol. 58, no. 12, pp. 1195–1199, 1990.